



HAL
open science

Characterization of water retention, compressibility and swelling properties of a pellet/powder bentonite mixture

Agustín Molinero Guerra, Yu-Jun Cui, Yong He, Pierre Delage, Nadia Mokni, Anh Minh A.M. Tang, Patrick Aïmediu, Michel Bornert, Frédéric Bernier

► To cite this version:

Agustín Molinero Guerra, Yu-Jun Cui, Yong He, Pierre Delage, Nadia Mokni, et al.. Characterization of water retention, compressibility and swelling properties of a pellet/powder bentonite mixture. *Engineering Geology*, 2019, 248, pp.14-21. 10.1016/j.enggeo.2018.11.005 . hal-01982177

HAL Id: hal-01982177

<https://hal.science/hal-01982177v1>

Submitted on 1 Feb 2024

HAL is a multi-disciplinary open access archive for the deposit and dissemination of scientific research documents, whether they are published or not. The documents may come from teaching and research institutions in France or abroad, or from public or private research centers.

L'archive ouverte pluridisciplinaire **HAL**, est destinée au dépôt et à la diffusion de documents scientifiques de niveau recherche, publiés ou non, émanant des établissements d'enseignement et de recherche français ou étrangers, des laboratoires publics ou privés.



Distributed under a Creative Commons Attribution - NonCommercial - NoDerivatives 4.0 International License

1 **Characterization of water retention, compressibility and swelling**
2 **properties of a pellet/powder bentonite mixture**

3 Agustín Molinero Guerra^{1,3}, Yu-Jun Cui¹, Yong He², Pierre Delage¹, Nadia Mokni³, Anh
4 Minh Tang¹, Patrick Aïmedieu⁴, Michel Bornert¹, Frédéric Bernier⁵

5 ¹Ecole des Ponts ParisTech, Laboratoire Navier, France

6 ²Central South University, School of Geosciences and Info-Physics, China

7 ³Institut de Radioprotection et de Sûreté Nucléaire (IRSN), France

8 ⁴Laboratoire Navier, UMR 8205, ENPC, IFSTTAR, CNRS, UPE, France

9 ⁵Agence Fédérale de Contrôle Nucléaire (AFCN), Belgium

10
11
12
13
14
15
16
17
18
19

20 **Corresponding author:**

21 Prof. Yu-Jun CUI

22 *Ecole des Ponts ParisTech*

23 6-8 av. Blaise Pascal, Cité Descartes, Champs-sur-Marne

24 F-77455 Marne - la - Vallée cedex - France

25 Telephone: +33 1 64 15 35 50

26 Fax: +33 1 64 15 35 62

27 E-mail: yu-jun.cui@enpc.fr

28
29
30

31 **Abstract:**

32 The water retention, compressibility and swelling properties of a pellet/powder bentonite
33 mixture were investigated in the laboratory. The water retention capacity was determined under
34 constant-volume condition using a specially designed cell allowing vapor exchange in all
35 directions; suction controlled oedometer tests were carried out for the compressibility
36 investigation; both constant-volume and swell-consolidation methods were applied for the
37 swelling pressure determination. The vapor equilibrium technique was used for suction control.
38 Comparable results were found for the water retention capacity of the pellet/powder mixture
39 determined under constant-volume condition and one single pellet under free swelling condition
40 for suctions higher than 4 MPa, suggesting that the suction was mainly controlled by the micro-
41 pores inside the pellets/powder grains and the swelling of the clay particles was accommodated
42 by the existing macro-pores. On the contrary, at lower suctions, the constant-volume conditions
43 gave rise to a lower water retention capacity for the mixture, indicating the restricted clay
44 particle swelling after the filling-up of the existing macro-pores. Oedometer compression
45 curves revealed a different behavior for low and high suctions: at high suctions, the volume
46 change behavior was governed by the pellets rearrangement combined with possible pellets
47 crushing upon loading. By contrast, at low suctions, the mixture lost its initial granular structure
48 during suction decrease; thus, the volume change behavior became similar to that of compacted
49 bentonite. Compared to compacted bentonite, the pellet/powder mixture showed a lower yield
50 stress. A lower value of swelling pressure was found with the constant-volume method,
51 confirming the limitation of the swell-consolidation method in determining soil swelling
52 pressure.

53

54 **Keywords:** pellet/powder bentonite mixture; laboratory testing; initial heterogeneity; water
55 retention; swelling; compressibility

57 **1. Introduction**

58 The design of most deep geological repositories for high level radioactive wastes (HLW) is
59 based on the multi-barrier concept which involves the natural host rock and engineered barriers
60 (Sellin and Leupin, 2013). In this design concept, bentonite-based materials are used to
61 construct buffers, backfills and seal plugs of disposal galleries and access shafts to ensure
62 isolation of the waste from the environment. In particular, mixtures made up of bentonite
63 powder and pellets are considered as a promising candidate sealing material because of its
64 particular properties. In addition to their low permeability, high swelling capacity and high
65 radionuclide migration retardation properties, the pellet/powder mixture exhibits operational
66 advantages in terms of emplacement and avoids the formation of technological gaps between
67 the host rock and the seal plug. Once installed in the repository, the pellet/powder mixture will
68 undergo both hydraulic and mechanical loadings: infiltration of host rock pore water and
69 mechanical confinement imposed by the surrounding rocks. In this context, to ensure the
70 stability of the storage structure, thus the safety of the disposal system, it is of paramount
71 importance to well understand the hydro-mechanical behavior of unsaturated bentonite
72 pellet/powder mixture. For this purpose, the French Institute for Radiation Protection and
73 Nuclear Safety (IRSN) launched the SEALEX project, which consisted of a series of in situ
74 experiments in the Underground Research Laboratory (URL) in Tournemire, France (Mokni
75 and Barnichon, 2016; Mokni, 2016). This project aimed at investigating the long-term hydraulic
76 performance of sealing systems in normal and critical scenarios, with different sealing plug
77 configurations (pre-compacted or field compacted sand/bentonite mixtures, pellet/powder
78 bentonite mixtures). In parallel to the in situ experiments, mock-up tests were also carried out
79 on compacted sand/bentonite blocks (Wang et al., 2012; Saba et al., 2014; Mokni, 2016). The
80 swelling pressure of compacted sand/bentonite blocks was also determined by Wang et al.

81 (2013a). The results confirmed the dominating role of the block dry density, identified by many
82 researchers (Börgesson et al., 1996; Dixon et al., 1996; Lloret et al., 2003; Villar, 2005; Gens
83 et al., 2011; Villar et al., 2012; Schanz and Al-Badran, 2014). Further examination showed that
84 sand in the mixture did not contribute to the swelling pressure; it was the dry density of
85 bentonite contained in the mixture that defined the final swelling pressure of the sand/bentonite
86 mixture (Wang et al., 2012; Saba et al., 2014), in agreement with the results obtained by
87 previous researchers (e.g. Villar and Rivas, 1994; Karnland et al., 2008). The well-established
88 relationship between final swelling pressure and bentonite dry density constituted a helpful tool
89 in interpreting the field observation in the SEALEX project (Wang et al., 2013a).

90 As opposed to the compacted bentonite-based blocks, the pellet/powder bentonite mixture has
91 been scarcely investigated in the laboratory. Hoffmann et al. (2007) performed different tests
92 on mixtures of different-size pellets of Febex bentonite at different dry densities considered
93 within the Engineered Barrier (EB) project. An important finding was the progressive decrease
94 of water permeability induced by the clogging of the large inter-pellet pores due to granule
95 swelling and the development of both swelling strain and pressure upon wetting. Imbert and
96 Villar (2006) investigated the hydro-mechanical behavior of a 50/50 FoCa bentonite
97 pellet/powder mixture by a series of infiltration tests. They concluded that the mixture became
98 homogeneous with a swelling pressure equal to that of a bentonite powder compacted at the
99 same dry density once full saturation was reached.

100 In this study, the water retention capacity and the swelling and compressibility properties of a
101 80/20 pellet/powder MX80 bentonite mixture were investigated. Firstly, the water retention
102 curve (WRC) was determined by following a wetting path under constant-volume conditions
103 using a specially designed cell with vapor exchange allowed in all directions. This curve was
104 compared to that of a single pellet of bentonite swelling under free swelling conditions.
105 Secondly, a series of suction controlled oedometer tests were performed to investigate the

106 compressibility properties of the mixture. The swelling behavior of the mixture after following
107 a wetting-drying path was also studied in oedometer. Finally, the swelling pressure was
108 investigated using both constant-volume and swell-consolidation methods. Emphasis was put
109 on the size of samples due to the strong heterogeneous nature of the material with large pellets.
110 The results obtained allowed the main hydro-mechanical properties of the bentonite
111 pellets/powder mixture used in the SEALEX project to be characterized, providing relevant
112 parameters for the numerical analysis of the field infiltration experiments involving this
113 mixture.

114 **2. Materials and methods**

115 **2.1. Materials**

116 The investigated material was a mixture of pellet/powder of MX80 bentonite at a proportion of
117 80/20 in dry mass. The MX80 bentonite came from Wyoming, USA, and had a smectite content
118 of 80%, other non-clayey inclusions being quartz, calcite and pyrite. The cation exchange
119 capacity (CEC) was 98 meq/100g, with Na⁺ as major exchangeable cation, with a value of 52
120 meq/100g (1.2 meq/100g for K⁺, 10 meq/100g for Mg²⁺ and 37 meq/100g for Ca²⁺). The liquid
121 limit was 560%, the plastic limit was 62% and the unit mass of solid was 2.77 Mg/m³ (Saba et
122 al., 2014).

123 Pellets were produced in the Laviosa-MPC company by instantaneously compacting MX80
124 bentonite in a mould of 7 mm in diameter and 7 mm in height. A zoom on a single pellet is
125 shown in Figure 1. The fabrication water content was $w = 6.0 \pm 1.0\%$ and the dry density was
126 $\rho_d = 2.06 \pm 0.06 \text{ Mg/m}^3$, corresponding to a void ratio $e = 0.30 \pm 0.07$. The pellets were stored
127 in the laboratory in a hermetic plastic box at 20°C. The initial suction ($s = 135 \pm 3 \text{ MPa}$) was
128 measured in the laboratory with a chilled mirror dew point hygrometer (Decagon WP4C), at an
129 initial water content $w = 7.2 \pm 1.0\%$ (determined after oven-drying at 105°C), slightly higher

130 than the fabrication one due to the water adoption from air after fabrication (Molinero Guerra
131 et al., 2017). Note that the WP4C measures corresponded to total suction, including the osmotic
132 suction.

133 The MX80 bentonite powder was produced by crushing pellets just after their fabrication. The
134 maximum size of grains was 2 mm and the portion of the grains smaller than 80 μm was 5%.
135 An initial water content of $3.2 \pm 1.0\%$ was found in the laboratory by oven-drying at 105°C for
136 24 h, corresponding to an initial suction $s = 191$ MPa (measured with WP4C). This water
137 content was quite low compared to the fabrication water content ($6.0 \pm 1.0\%$), suggesting loss
138 of some water during the pellets crushing operation. More details about the initial state of the
139 material can be found in Molinero Guerra et al. (2017).

140 **2.1. Sample preparation**

141 All the results presented in this study were obtained by performing laboratory tests on the
142 pellet/powder bentonite mixture. The mixture was prepared by following the first protocol
143 presented in Molinero Guerra et al. (2017) to obtain a relatively homogeneous pellet/powder
144 distribution. It consisted in filling the cell by packets corresponding to one layer of pellets
145 spread over the base of the cylinder, with the corresponding amount of powder, respecting the
146 proportion of 80-pellets/20-powder. The global dry initial density of the mixture thus prepared
147 was 1.49 Mg/m³.

148 In order to better understand the initial pellet/powder distribution, microfocus X-ray computed
149 tomography observations were made on the mixture at its initial state. A vertical slice is
150 presented in Figure 2. The dimensions of the observed sample were 120 mm in height and 60
151 mm in diameter. It appears that even though a special protocol was followed, it was difficult to
152 perfectly control the homogeneity of the sample. Indeed, the grains of powder were not
153 uniformly distributed within the sample, and inter-pellet voids could be clearly identified. The

154 sample, placed between two porous stones, presented larger inter-pellet voids close to the top
155 porous stone and no grains of powder were observed in this zone. Therefore, this material was
156 characterized by a strong heterogeneity at its initial state, which is an important aspect to take
157 into account while further analyzing the global hydro-mechanical behavior of the sample. This
158 initial heterogeneity was investigated in depth by Molinero Guerra et al. (2017).

159 The samples used for the present study were prepared in the same manner, but with a height of
160 35 mm. This height corresponded to 5 times the height of a single pellet and it was believed
161 that such dimensions constituted a representative volume of the pellet/powder mixture. This
162 ratio of sample size to maximum grain size was also adopted by Duong et al. (2013) when
163 investigating the mechanical behavior of a mixture of coarse and fine soils.

164 **2.2. Experimental methods**

165 *2.2.1. Water retention properties*

166 The water retention curve (WRC) of the pellet/powder bentonite mixture under constant-
167 volume conditions was determined on samples of 50 mm in diameter. A special device
168 presented in Figure 3 was designed for this purpose. The pellet/powder mixture was placed into
169 a rigid stainless steel cell that was designed to allow vapor exchanges not only through the two
170 metallic porous disks on both top and bottom of the sample, but also through a cylindrical
171 porous disk on the lateral surface of the sample. This design was expected to significantly
172 accelerate the hydration of the sample by vapor equilibrium technique, essential for low-
173 permeability materials like the studied swelling MX80 bentonite. The mass of sample was
174 regularly measured. In a standard fashion, equilibrium was considered once the mass changes
175 became insignificant. For each pellet/powder mixture, once equilibrium was reached, three
176 measures were performed for both the water content by oven drying and the suction with WP4C.
177 The mean values were considered in the further analyses.

178 In parallel, the water retention curve under free swelling conditions for a single pellet of
179 bentonite was obtained. To this end, pellets were hydrated under several values of suction from
180 their initial state by vapor equilibrium technique. For the pellet/powder mixture, zero suction
181 was applied by injecting deionized water into the cell under a low pressure corresponding to a
182 water column height of about 200 mm.

183 *2.2.2. Compressibility properties – suction controlled oedometer tests*

184 Controlled suction oedometer compression tests were performed on samples of 35 mm in height
185 and 50 mm in diameter by circulating vapor at controlled relative humidity through the base of
186 the sample as shown in Figure 4 (tests SCO1, SCO2 and SCO3 presented in Table 1). In order
187 to investigate the mechanical behavior of the mixture in a relatively large range of load, a high
188 pressure oedometer was used allowing application of vertical stresses as high as 50 MPa
189 (Marcial et al., 2002). This oedometer was previously calibrated using a force transducer in
190 order to ensure the accuracy of the imposed pressures. As opposed to other suction values, zero
191 suction was imposed by circulating deionized water. Vertical displacement was monitored
192 using a digital micrometer (accuracy ± 0.001 mm). The temperature in the laboratory was
193 controlled at $20 \pm 0.5^\circ\text{C}$ during the experiments.

194 Time was allowed until swelling stabilized under the imposed value of suction and a low
195 vertical stress of 0.1 MPa. The stabilization was considered when the vertical displacement was
196 lower than 0.01 mm for, at least, 8 h. It is worth noting this criterion was defined based on the
197 French Standard AFNOR (1995) for oedometer compression test. The real swelling
198 stabilization might take much longer time. Three tests were carried out under three different
199 suctions (0 MPa, 9 MPa and 138 MPa). The test at 138 MPa suction (SCO1) was performed
200 without imposing the suction, assuming that the suction changes during loading-unloading were
201 negligible. In this case, the test was performed at constant water content. This assumption was
202 supported by the results of Gens et al. (1995) who measured the suctions of a soil compacted

203 under three different stresses and observed that on the dry side of optimum the soil suction was
204 almost the same, suggesting that inter-aggregate macro-pores were dry. Similarly, in this study,
205 the macro-pores of the pellets/powder mixture could be considered as dry at a suction as high
206 as 138 MPa. Thus, it is assumed that compression decreased the macro-pores but not the suction
207 of the mixture.

208 Loadings were performed in steps from 0.1 MPa. A new load equal to the double of the previous
209 one was applied (except the last loading step for sample SCO1) when the change of the vertical
210 displacement became insignificant (< 0.01 mm for 8 h according to AFNOR, 1995). The
211 maximums loads were 12.8 MPa for SCO2, SCO3 and SCO4 and 18 MPa for SCO1 because
212 of the higher stiffness of this latter due to its higher suction. After the loading process,
213 unloadings were performed in steps down to different load values.

214 2.2.3. *Swelling properties*

215 Three tests, SCO3, SCO4 and CV1 presented in Table 1, were performed in order to study the
216 swelling properties of the pellet/powder bentonite mixture. Both the constant-volume and
217 swell-consolidation methods were applied to determine the swelling pressure. To apply the
218 constant-volume method, a constant volume cell was used, which included three parts: (i) the
219 bottom part which contained a porous stone and a drainage system; (ii) the middle cell (70 mm
220 in inner diameter) which prevented any radial swelling, with two air outlets; (iii) the top part
221 including a total pressure sensor for monitoring the axial swelling pressure. The water inlet was
222 connected to a water reservoir placed at the same height of the cell, flooding the pellet/powder
223 mixture from the bottom. The saturation water used was a synthetic water (see Table 2 for the
224 receipt of preparation), which has the same chemical composition as the pore water of the
225 Callovo-Oxfordian claystone in the underground research laboratory of the French agency for
226 radioactive waste management (ANDRA) in Bure, France. In the swell-consolidation method,
227 the sample was hydrated under a low vertical load of 0.1 MPa until full swelling was achieved.

228 Then, it was compressed following a standard consolidation test procedure. The pressure
229 needed to compress the specimen back to its initial volume was defined as the swelling pressure
230 of the material (Basma et al., 1995; Abdullah and Mhaidib, 1998, 1999; Agus, 2005, Wang et
231 al. 2012).

232 **3. Experimental results**

233 *3.1. Water retention curve*

234 Figure 5 displays the evolution of water content with time for the pellet/powder mixture
235 equilibrated at different suctions. The special cell designed allowed the samples to reach water
236 content stabilisation quite quickly. This was because with the specially designed cell (Figure
237 3), the sample was completely surrounded by porous stones, which accelerated the vapor
238 exchange process. For all imposed suctions, the water content was stabilized after 30 days of
239 hydration, except for 4 MPa and 82 MPa. For $s = 4$ MPa, some technical problems occurred
240 during the test, and a constant water content value was found after 80 days. It is suspected that,
241 at this low suction, the hydration system failed after a certain time due to water condensation
242 in the pipes – cleaning intervention was necessary to solve the problem. The slight temperature
243 fluctuations of $\pm 0.5^{\circ}\text{C}$ in the laboratory during the experiments could cause this condensation.
244 For suction $s = 82$ MPa, it seems that water content was constant after 30 days; nevertheless, it
245 continued increasing slightly up to 90 days. For this value of suction, several problems were
246 found during wetting in the hydration system (blockage of the vapor circulation system) and
247 regular interventions were needed. It could be considered that this technique ran well for
248 suctions higher than or equal to 9 MPa. For lower suctions, problems related to condensation
249 in the pipes could be significant in the relatively long tests (more than 80 days). These problems
250 are to be solved in further studies, by placing the main system in water with temperature control
251 for example.

252 The water retention curves under constant (pellet/powder mixture) and free swelling conditions
253 (single pellet) for a wetting path are presented in Figure 6 in terms of water content versus
254 suction. It appeared that pellet and mixture had comparable water retention capacities when
255 suction was higher than 4 MPa, suggesting that the suction was governed by the micro-pores
256 within the pellets or powder grains. In addition, in the case of the mixture, the existing macro-
257 pores can accommodate the swelling of the clay particles. This is in agreement with the results
258 obtained by Yahia-Aissa et al. (2001) on compacted Foca 7 clay. It seems that the mixture had
259 a lower water retention capacity under constant-volume conditions for suctions lower than 4
260 MPa, since its water content at zero suction was 34.3%. This indicated the restriction effect on
261 the clay particles swelling, thus the water retention capacity. More data are needed in this range
262 of suction to confirm this conclusion. Figure 7 presents the suctions measured by WP4C versus
263 the imposed values by either vapor equilibrium technique (for non-zero suctions) or injecting
264 deionized water (for zero suction) for the pellet/powder mixture.

265 Some differences were found between the measured suction after equilibrium and the imposed
266 value by vapor equilibrium technique, in particular for zero suction. This could be due to the
267 stress release while dismantling the specimen, which led the suction to increase within the
268 mixture. This effect appeared more pronounced in the case of zero suction due to the highest
269 swelling pressure developed, which enhanced the stress release effect.

270 Pintado et al. (2009) concluded that, with the vapor equilibrium technique, it was difficult to
271 reach the same suction distribution inside the sample. From Figure 7, it appears that the suction
272 imposed and the suction measured were almost the same, indicating that in our case the uniform
273 suction distribution was reached thanks to the additional air flow through the lateral surface.
274 This shows the performance of the designed device.

275 3.2. *Controlled suction compression tests (SCO1, SCO2 and SCO3)*

276 Figure 8 presents the evolution of volumetric strain with time for tests SCO1, SCO2 and SCO3.
277 The test at 138 MPa of suction was performed without imposing suction. It was carried out at
278 constant water content conditions. As mentioned before, the suction can be reasonably
279 considered as constant in this test.

280 In test SCO3, the pellet/powder mixture was hydrated under 0.1 MPa by injecting deionized
281 water to impose zero suction. Equilibrium was reached after 1272 h (53 days), with a value of
282 21% of volumetric strain, corresponding to a void ratio of $e = 1.25$. The volumetric strain at
283 equilibrium was higher than the value obtained by Wang et al. (2012) for compacted
284 bentonite/sand mixture: 18% ($e = 0.97$). This could be explained by the higher swelling capacity
285 of the pellet/powder mixture without sand. In test SCO2 for 9 MPa suction applied by vapor
286 equilibrium technique, equilibrium was achieved after 1032 h (43 days), with a volumetric
287 strain of 9% ($e = 1.02$). A constant-volumetric strain was reached between 320 h and 430 h.
288 This is due to a problem in the hydration system that needed a cleaning intervention. After
289 430 h, the specimen continued swelling until reaching equilibrium. In test SCO1, no suction
290 was imposed as 138 MPa corresponded to the initial state of the pellet/powder mixture; a period
291 of 5 days was considered prior to loading in this case.

292 Once equilibrium was reached, the samples were submitted to loading/unloading at constant
293 suctions. For SCO3 (zero suction), on the whole, the evolution of volumetric strain in each
294 loading step showed typical consolidation features of fine-grained soils, in particular under high
295 loads. On the contrary, for SCO1 (138 suction) and SCO2 (9 MPa suction), the evolution curves
296 were rather characterized by the presence of almost instantaneous volumetric strains after each
297 loading. It was thus suspected that when suction was higher than 9 MPa, it was rather the
298 pellets/grains arrangement or crushing that governed the volume change behavior of the
299 mixture.

300 Test SCO4 was designed to study the volume change behavior upon wetting/drying in
301 oedometer. In this case, the pellet/powder mixture was submitted to a wetting-drying cycle at a
302 constant vertical stress of 0.1 MPa. In the first phase, the specimen was hydrated by injecting
303 deionized water during 1248 h (52 days) to reach equilibrium at zero suction (comparable to
304 the 1272 h for test SCO3). A volumetric strain of 23% ($e = 1.28$) was found at equilibrium.
305 Then, a suction of 262 MPa was imposed to the mixture. The volumetric strain decreased
306 drastically, reaching a value of 5% ($e = 0.87$) after 1375 h (57.3 days). A final value of 3% (e
307 $= 0.84$) was observed after 2311 h (96.3 days).

308 Once equilibrated at the imposed suctions, the pellet/powder mixtures were submitted to
309 compression at constant suctions. The results are displayed in Figure 9 in terms of void ratio
310 with respect to vertical stress. The initial void ratio values were different due to the different
311 swellings under different suctions. In a standard fashion, the compression curves were
312 characterized by an initial linear part with low compressibility (that could be considered as the
313 pseudo-elastic domain) followed by a second part with higher compressibility (that could be
314 considered as the plastic domain). Finally, the third part, corresponding to the unloading,
315 exhibited the same trend as the elastic domain, as only elastic deformations were expected. For
316 test SCO3 where zero suction was applied, the unloading path could also be considered as bi-
317 linear.

318 The swelling pressure of the pellet/powder mixture could be determined by the swell-
319 consolidation method using the results from test SCO3. As it was explained previously, the
320 swelling pressure of the material corresponded to the vertical stress needed to compress the
321 sample to its initial volume. The obtained value was $\sigma_s = 7.1$ MPa ($e = 0.859$).

322 3.3. *Swelling under constant-volume conditions (CVI)*

323 The swelling behavior of the pellet/powder bentonite mixture under constant-volume
324 conditions was investigated by following the evolution of the axial swelling pressure during
325 hydration (CV1 in Table 1). The results are displayed in Figure 10. Two rates of increase of
326 axial swelling pressure could be distinguished from the beginning of the hydration process: the
327 first one corresponded to a period from the beginning of the hydration up to 20 days, when
328 swelling pressure reached 0.43 MPa. Then, the pressure continued increasing at a different rate,
329 until 45 days of hydration. At this moment, the swelling pressure reached 0.8 MPa. Afterwards,
330 a slight increase was observed, finally reaching 0.87 MPa after 440 days. Nevertheless, the
331 swelling pressure continued increasing, which means that the sample was not completely
332 stabilized, even though the rate of increase was quite low compared to those observed before.
333 The value of pressure observed after 440 days (0.87 MPa) was significantly lower than the
334 value obtained by applying the swell-consolidation method on the consolidation curve (7.1
335 MPa).

336 **Discussion**

337 The swell-consolidation and constant-volume method revealed different values of swelling
338 pressure: the swell-consolidation method provided 7.1 MPa, whereas a value of 0.87 MPa was
339 found with the constant-volume method. This was common results and Wang et al. (2012)
340 explained that by the coupling between the microstructure deformation and the macrostructure
341 deformation, combined to the effect of friction.

342 Cui et al. (2013) carried out oedometer tests with loading/unloading/reloading on natural stiff
343 Ypresian clays (YPClay). They concluded that each unloading/reloading curve could be
344 satisfactorily considered as bi-linear with a small and a larger slope separated by a threshold
345 vertical stress. This stress was found, through hydrations tests under constant volume
346 conditions, to be the swelling pressure corresponding to the void ratio just before the unloading

347 or reloading. By applying this approach to the pellet/powder mixture at zero suction (SCO3),
348 with the consideration of the unloading path as bilinear, a swelling pressure of 4.2 MPa
349 (threshold vertical stress) would be obtained, corresponding to a void ratio $e = 0.72$ (dry density
350 $\rho_d = 1.61 \text{ Mg/m}^3$). This value was comparable with that estimated by the method of Wang et al.
351 (2012): a value of 4.15 MPa of swelling pressure was found at a dry density of 1.49 Mg/m^3 .
352 This showed that the true swelling pressure of the mixture should be lower than that determined
353 by the swell-consolidation method, because the value would correspond to the point separating
354 the two parts of unloading curve, thus below the consolidation curve.

355 Further analysis of the swelling pressure evolution with time displayed in Figure 10 revealed
356 the processes governing the structural changes of the pellet/powder mixture while wetting. At
357 the very beginning of the test with wetting from the bottom, the observed swelling pressure and
358 the corresponding rate of increase were due to the pellets located at the top of the sample, where
359 the suction was still high. After a period of 20 days, a second rate of increase higher than the
360 first one was observed. The reason was that water has arrived to pellets or powder grains located
361 at the top of the sample at this state; thus, the involved pellets and powder grains started swelling
362 and the pressure increased accordingly. It was suspected that all inter-pellet/grain voids were
363 filled with swollen bentonite after 40 days of hydration, as the rate of increase of swelling
364 pressure decreased. However, the rate was not equal to zero, meaning that the specimen was
365 not homogeneous. Taking into account the relationship proposed by Wang et al. (2013a)
366 between the swelling pressure and the dry density of bentonite, a final value of 4.15 MPa of
367 swelling pressure was found. Obviously, the swelling pressure of 0.87 MPa obtained by the
368 constant method was quite far from this value. Molinero Guerra et al. (2018) performed an
369 infiltration test on the same mixture with the same global dry density (1.49 Mg/m^3) using a
370 metallic column (60 mm in diameter and 120 mm in height) equipped with a force transducer
371 for the axial swelling pressure measurement and several total pressure transducers for the radial

372 swelling pressure measurements at different positions (20 mm, 40 mm, 60 mm, 80 mm and
373 100 mm from the bottom of sample). Water infiltration was allowed from both the top and the
374 bottom of sample. They observed an axial swelling pressure of 2.5 MPa after 845-day
375 infiltration, also lower than the expected value (4.15 MPa). The radial pressures at 20 mm, 40
376 mm, 60 mm, 80 mm were almost the same, around 4 MPa. By contrast, the value at 100 mm
377 was lower, around 3 MPa. In addition, the swelling pressures were developed mainly during
378 the first 100 days, the variations after 100 days appearing negligible. They attributed the
379 difference between the radial swelling pressures by the heterogeneity of the sample: a higher
380 swelling pressure was expected at a position where the local dry density was greater. They
381 explained the lower axial pressure by the effect of friction between the sample and the column
382 wall, as also identified by Saba et al. (2014). Indeed, the expected sample homogenization
383 process implied the local movements of bentonite particles. Thus, the wall friction could be
384 mobilized even in constant-volume condition. The results obtained in this study showed that
385 even for a sample of 35 mm height, the effect of cell wall friction was significant, hampering
386 or slowing down the sample homogenization process.

387 The results from test SCO4 allowed the reversibility of swelling of the pellet/powder mixture
388 to be investigated. After wetting under zero suction, the sample was dried by imposing $s = 262$
389 MPa. The results showed a drastic decrease of volumetric strain, reaching a final value of 3%.
390 This suggested that plastic swelling strain occurred upon wetting under zero suction, as shown
391 in Figure 11. This was probably due to pellets fissuring upon wetting. Wang et al. (2013b) also
392 reported the fissuring phenomenon for compacted bentonite/sand mixture upon wetting.
393 Compared to test SCO3, a slightly higher volumetric strain was reached in test SCO4,
394 suggesting a certain effect of the pellet/powder distribution that is specific for each sample. The
395 final points of tests SCO1, SCO2 and SCO3 appeared well aligned, defining a wetting line. This

396 line was below the drying line estimated from test SCO4. The difference between the two lines
397 was larger at higher suction.

398 The evolution of the yield stress with suction is presented in Figure 12, together with the values
399 obtained by Marcial et al. (2003) and Wang et al. (2013b) for compacted bentonite with initial
400 void ratio of 0.559 and compacted bentonite/sand mixture with initial void ratio of 0.635,
401 respectively. A good coincidence was observed for compacted bentonite and the pellet/powder
402 mixture at zero suction. For other values of suction, in a standard fashion, the yield stress
403 increased as suction increased. However, this phenomenon was not clear for the pellet/powder
404 mixture: a much lower yield stress value was obtained. A possible explanation is as follows:
405 for non-zero suctions, the pellet/powder mixture did not completely lose its initial granular
406 mixture; thus, the deformations were essentially governed by the rearrangement and possible
407 crushing of pellets while loading. These deformations were of plastic nature. However, in the
408 case of zero suction, the mixture entirely lost its granular structure; thus, the volume change
409 behavior was comparable to that of a common compacted bentonite. This observation was
410 supported by analyzing the evolution of volumetric strain with time: at 138 MPa and 9 MPa of
411 suctions, the volumetric strains decreased almost instantaneously while loading; however, at
412 zero suction, the decrease rate of volumetric strain was clearly lower than those observed at
413 other suctions, because the pellets lost their granular structure in that case.

414 **4. Conclusion**

415 The water retention, compressibility and swelling properties of a 80-pellet/20-powder bentonite
416 mixture were investigated through the water retention tests under free (pellet) and constant-
417 volume (mixture) conditions, the suction controlled oedometer tests and the hydraulic tests on
418 samples at a dry density of 1.49 Mg/m³.

419 The new cell designed for the WRC determination under constant-volume condition allowed
420 the vapor exchange in all directions, which significantly accelerated the hydration process.

421 Similar water retention properties were observed for pellet/powder mixture under constant-
422 volume condition and single pellet under free swelling condition at suction higher than 4 MPa,
423 indicating that the suction was mainly controlled by the micro-pores inside the pellets or powder
424 grains, and the swell of clay particles was accommodated by existing macro-pores in the
425 mixture. On the contrary, at lower suctions, constant-volume condition defined a lower water
426 retention capacity, showing the restriction effect on clay particles swelling and thus their
427 hydration. Note that more tests are needed to complete the data in the range of suctions lower
428 than 4 MPa.

429 The investigation of the compressibility properties revealed lower values of yield stress than
430 the common bentonite mixtures, except for the specimen hydrated at zero suction. This is due
431 to the granular structure in the case of non-zero suction where the volume change behavior was
432 suspected to be governed by the rearrangement and crushing of pellets, and the loss of the
433 granular structure in the case of zero suction.

434 The irreversibility of the volumetric strain was evidenced by imposing a wetting-drying cycle
435 to the pellet/powder mixture under constant loading. This was probably due to the pellets/grains
436 fissuring upon wetting.

437 Different swelling pressure values were obtained by applying different methods. A higher
438 swelling pressure was obtained with the swell-consolidation method. Further analysis based on
439 the method proposed by Cui et al. (2013) showed that the swell-consolidation systematically
440 overestimates the swelling pressure because for a given density the swelling pressure must be
441 lower than the corresponding pressure on the consolidation curve: the swelling pressure
442 corresponded to the point separating the two parts of unloading curve, thus below the

443 consolidation curve. Nevertheless, the swelling pressure determined by the constant-volume
444 method seemed quite low (0.87 MPa) with respect to the expected one (4.15 MPa). This could
445 be attributed to the effect of cell wall friction because the expected sample homogenization
446 process implied the local movements of bentonite particles, thereby mobilizing the cell wall
447 friction even in constant-volume condition and with a sample of limited height (35 mm). The
448 cell wall friction would hamper or slow down the sample homogenization process.

449 **References**

- 450 Abdullah, I., Mhaidib, A., (1998). Prediction of swelling potential of an expansive shale.
451 Proceedings Of The Second International Conference On unsaturated soils. 27–30
452 August. Beijing, China, vol. 1.
- 453 Abdullah, I., Mhaidib, A., (1999). Swelling behaviour of expansive shales from the middle
454 region of Saudi Arabia. *Geotechnical and Geological Engineering* 16 (4), 291–307.
- 455 AFNOR, (1995). Sols : reconnaissance et essais: essai de gonflement à l'oedomètre,
456 détermination des déformations par chargement de plusieurs éprouvettes. XP P 94-091
- 457 Agus, S., (2005). An Experimental study on hydro-mechanical characteristics of com-
458 pacted bentonite-sand mixtures. PhD thesis. Weimar.
- 459 Basma, A.A., Al-Homoud, A.S., Husein, A., (1995). Laboratory assessment of swelling pres-
460 sure of expansive soils. *Applied Clay Science* 9 (5), 355–368.
- 461 Börgesson, L., Karnland, O. and Johannesson, L. E., (1996). Modelling of the physical
462 behaviour of clay barriers close to water saturation. *Engineering Geology* 41, No. 1–4,
463 127–144.
- 464 Cui, Y. J., Nguyen, X. P., Tang, A. M., and Li., X. L., (2013). An Insight into the
465 Unloading/reloading Loops on the Compression Curve of Natural Stiff Clays. *Applied*
466 *Clay Science* 83-84: 343–48.
- 467 Dixon, D. A., Gray, M. N. and Graham, J., (1996). Swelling and hydraulic properties of
468 bentonites from Japan, Canada and the USA. *Environmental Geotechnics* 1, 43–48.
- 469 Duong, T. V., Tang, A. M., Cui, Y. J., Trinh, V. N., Dupla, J. C., Calon, N., Canou, J., and
470 Robinet, A. (2013). Effects of fines and water contents on the mechanical behavior of
471 interlayer soil in ancient railway sub-structure, *Soils Found.*, vol. 53, no. 6, pp. 868–878.
- 472 Gens, A., Alonso, E.E., Suriol, J. & Lloret, A. (1995). Effect of structure on the volumetric
473 behaviour of a compacted soil. Proc. of 1st conference on unsaturated soils. vol. 2, pp.
474 83-88.

- 475 Gens, A., Vallejan, B., Sánchez, M., Imbert, C., Villar, M.V. and Van Geet, M., (2011).
476 Hydro mechanical Behavior of a Heterogenous Compacted Soil: Experimental
477 Observations and Modelling.
- 478 Hoffmann, C., Alonso, E.E. & Romero, E., (2007). Hydro-mechanical behaviour of bentonite
479 pellet mixtures. *Physics and Chemistry of the Earth*, 32(8-14), pp.832–849.
- 480 Imbert, C. & Villar, M.V., (2006). Hydro-mechanical response of a bentonite pellets/powder
481 mixture upon infiltration. *Applied Clay Science*, 32(3-4), pp.197–209.
- 482 Karnland, O., Nilsson, U., Weber, H., Wersin, P., (2008). Sealing ability of Wyoming
483 bentonite pellets foreseen as buffer material – laboratory results. *Physics and Chemistry
484 of the Earth, Parts A/B/C* 33, S472–S475.
- 485 Lloret, A., Villar, M. V., Sánchez, M., Gens, A., Pintado, X. and Alonso, E. E., (2003).
486 Mechanical behaviour of heavily compacted bentonite under high suction changes.
487 *Géotechnique* 53, No. 1, 27–40.
- 488 Marcial, D., Delage, P., Cui, Y.J., (2002). On the high stress compression of bentonites.
489 *Canadian Geotechnical Journal* 39, 812–820.
- 490 Marcial, D., (2003). Comportement hydromécanique et microstructural des matériaux de
491 barrière ouvragée, thèse. ENPC Paris, France.
- 492 Mokni, N. & Barnichon, J.D., (2016). Hydro-mechanical analysis of SEALEX in situ tests-
493 Impact of technological gaps on long term performance of repository seals. *Engineering
494 Geology*, 205, pp. 81-92.
- 495 Mokni, N., (2016). Analysis of hydro-mechanical behaviourbehavior of compacted
496 bentonite/sand mixture using a double structure formulation. *Environ Earth Sci* (2016)
497 75: 1087.
- 498 Molinero-Guerra, A., Mokni, N., Delage, P., Cui, Y. J., Tang, A. M., Aïmedieu, P., Bernier,
499 F. and Bornert, M., (2017). In-depth characterisation of a mixture composed of
500 powder/pellets MX80 bentonite. *Applied Clay Science*, 135, pp. 538-546.
- 501 Molinero-Guerra, A., Cui, Y. J., Mokni, N., Delage, P., Bornert, M., Aïmedieu, P., Tang, A.
502 M., Bernier, F. and (2018). Investigation of the hydro-mechanical behaviour of a
503 pellet/powder MX80 betonite mixture using an infiltration column. *Engineering
504 Geology*, 243, pp. 18-25.
- 505 Pintado, X., Lloret, A., Romero, E., (2009). Assessment of the use of the vapour equilibrium
506 technique in controlled-suction tests. *Canadian Geotechnical Journal* 46: 411-123
- 507 Saba, S., Cui, Y.J., Tang, A.M., and Barnichon, J.D., (2014). Investigation of the swelling
508 behaviour of compacted bentonite–sand mixture by mock-up tests. *Canadian
509 Geotechnical Journal*, 51(12), pp.1399–1412.
- 510 Sellin, P., and Leupin, O. X., (2013). The use of clay as an engineered barrier in radioactive-
511 waste management – a review. *Clays and Clay Minerals* 61, No. 6, 477–498.

- 512 Schanz, T. and Al-Badran, Y., (2014). Swelling pressure characteristics of compacted Chinese
513 Gaomiaozi bentonite GMZ01. *Soils and Foundations* 54, No. 4, 748–759.
- 514 Villar, M.V., Rivas P. (1994). Hydraulic properties of montmorillonite-quartz and saponite-
515 quartz mixtures. *Applied Clay Science* 9, 1-9
- 516 Villar, M.V. (2005). MX-80 Bentonite. Thermo-Hydro-Mechanical Characterization
517 Performed at CIEMAT in the Context of Prototype Project. Ciemat technical report
518 1053. Madrid, Spain.
- 519 Villar, M. V., Gómez-Espina, R. and Guitiérrez-Nebot, L., (2012). Basal spacings of smectite
520 in compacted bentonite. *Applied Clay Science* 65–66, 95–105.
- 521 Wang, Q., Tang, A. M., Cui, Y. J., Delage, P., and Gatmiri, B., (2012). Experimental study on
522 the swelling behaviour of bentonite/claystone mixture. *Eng. Geol.*, vol. 124, no. 1, pp.
523 59–66.
- 524 Wang, Q., Tang, A.M., Cui, Y.J., Barnichon, J.D. and Ye, W.M., (2013a). A comparative stud
525 on the hydro-mechanical behaviour of compacted bentonite/sand plug based on
526 laboratory and field infiltration tests. *Eng. Geol.* 162, 79–87.
- 527 Wang, Q., Tang, A.M., Cui, Y.J., Barnichon, J.D. Ye, W.M., (2013b). Investigation of the
528 hydro-mechanical behaviour of compacted bentonite/sand mixture based on the BExM
529 model. *Computer and Geotechnics* 54, 46-52.
- 530 Yahia-Aissa, M., Delage, P., Cui, Y.J., (2001). Suction–water relationship in swelling clays.
531 *Clay Science for Engineering*. In: Adachi, K., Fukue, M. (Eds.), *Proceedings of the IS-*
532 *Shizuoka International Symposium on Suction, Swelling, Permeability and Structure of*
533 *Clays*. Shizuoka, Japan Balkema, pp. 65–68.
- 534

535 **List of Tables**

536 Table 1. Test program for investigating the compressibility and swelling properties of pellet/powder
537 bentonite mixture

538 Table 2. Receipt for preparing the synthetic water.
539

540

541 **List of Figures**

542 Figure 1. Pellet at its initial state.

543 Figure 2. Vertical slice on the investigated pellet/powder bentonite mixture obtained by μ -CT
544 observations - Resolution: 50 $\mu\text{m}/\text{voxel}$.

545 Figure 3. Schematic view of the special cell designed for determining the water retention
546 curve under constant-volume conditions.

547 Figure 4. Experimental setup for suction-controlled oedometer tests.

548 Figure 5. Evolution of water content with time for the pellet/powder bentonite mixture
549 submitted to different suctions under constant-volume conditions.

550 Figure 6. Water retention properties under free swelling conditions and constant-volume
551 conditions.

552 Figure 7. Imposed suctions by vapour equilibrium technique versus measured suction after
553 equilibrium for the pellet/powder bentonite mixture.

554 Figure 8. Evolution of the volumetric strain with time in the oedometer tests SCO1, SCO2
555 and SCO3.

556 Figure 9. Void ratio versus vertical stress for tests SCO1, SCO2 and SCO3.

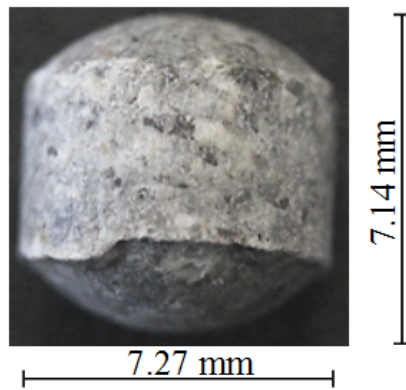
557 Figure 10. Evolution of axial swelling pressure with time in test CV1.

558 Figure 11. Volumetric strains measured at different suctions after equilibrium at the imposed
559 suction for the different tests.

560 Figure 12. Yield stress versus suction for compacted bentonite with initial void ratio of 0.559
561 (Marcial, 2003), compacted bentonite/sand mixture with initial void ratio of 0.635 (Wang et
562 al., 2013b) and pellet/powder mixture with initial void ratio of 0.859 (present work).
563

564

565

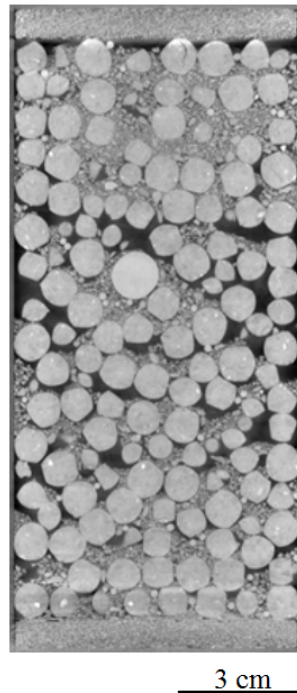


566

567

Figure 1. Pellet at its initial state.

568

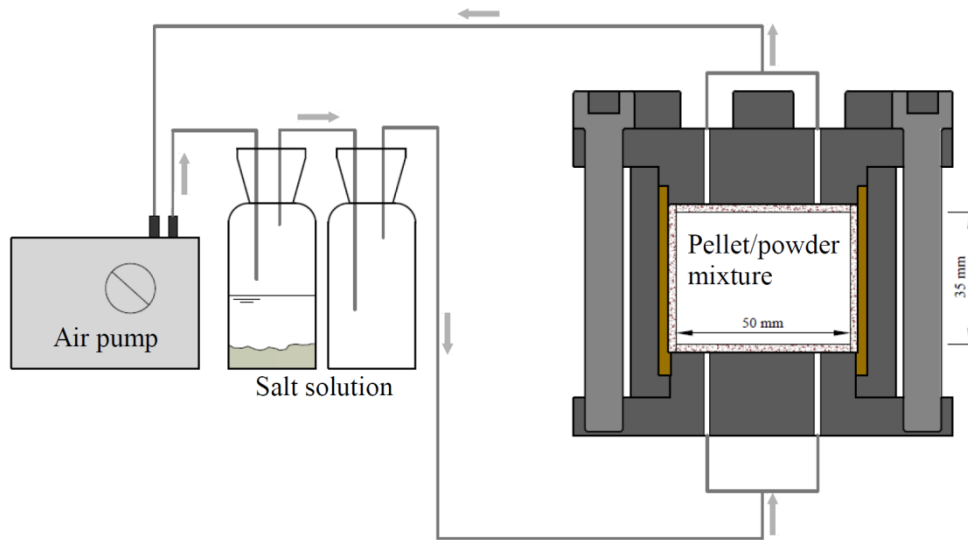


569

570

571

Figure 2. Vertical slice on the investigated pellet/powder bentonite mixture obtained by μ -CT observations - Resolution: 50 μ m/voxel.



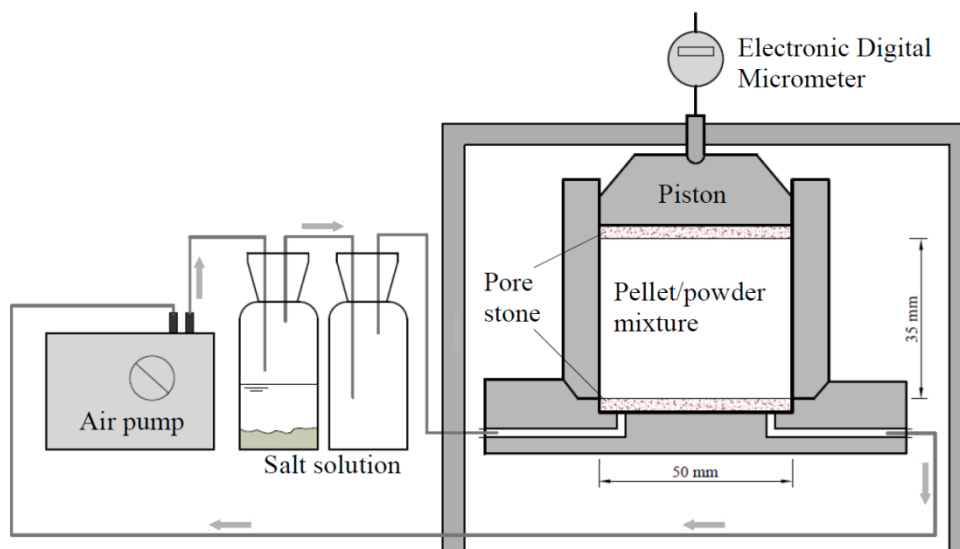
572

573

574

Figure 3. Schematic view of the special cell designed for determining the water retention curve under constant-volume conditions.

575



576

577

Figure 4. Experimental setup for suction-controlled oedometer tests.

578

579

580

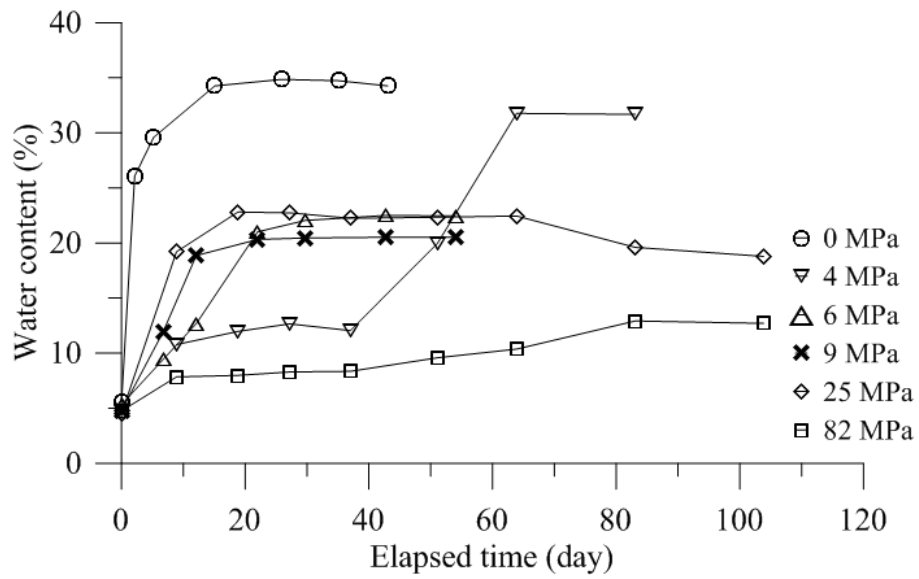
581

582

583

584

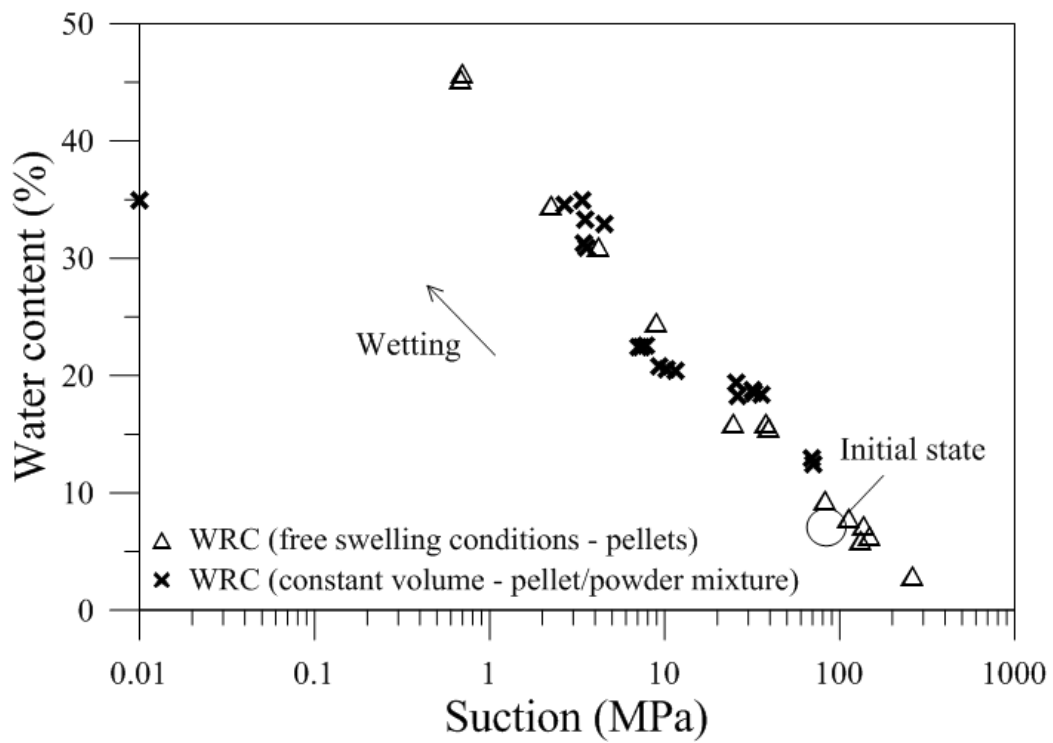
585



586

587 Figure 5. Evolution of water content with time for the pellet/powder bentonite mixture
 588 submitted to different suctions under constant-volume conditions.

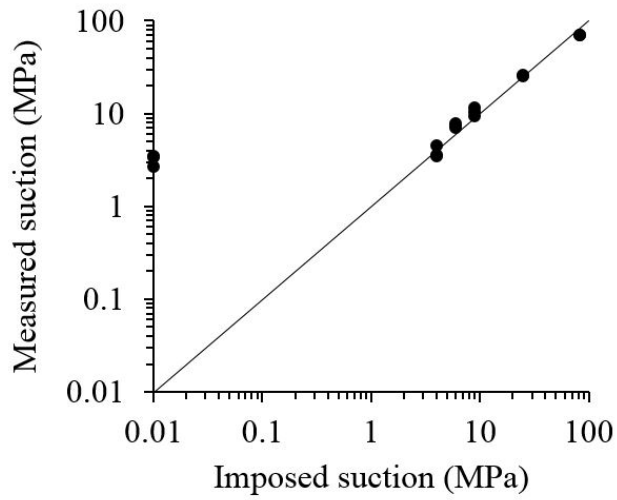
589



590

591 Figure 6. Water retention properties under free swelling conditions and constant-volume
 592 conditions.

593

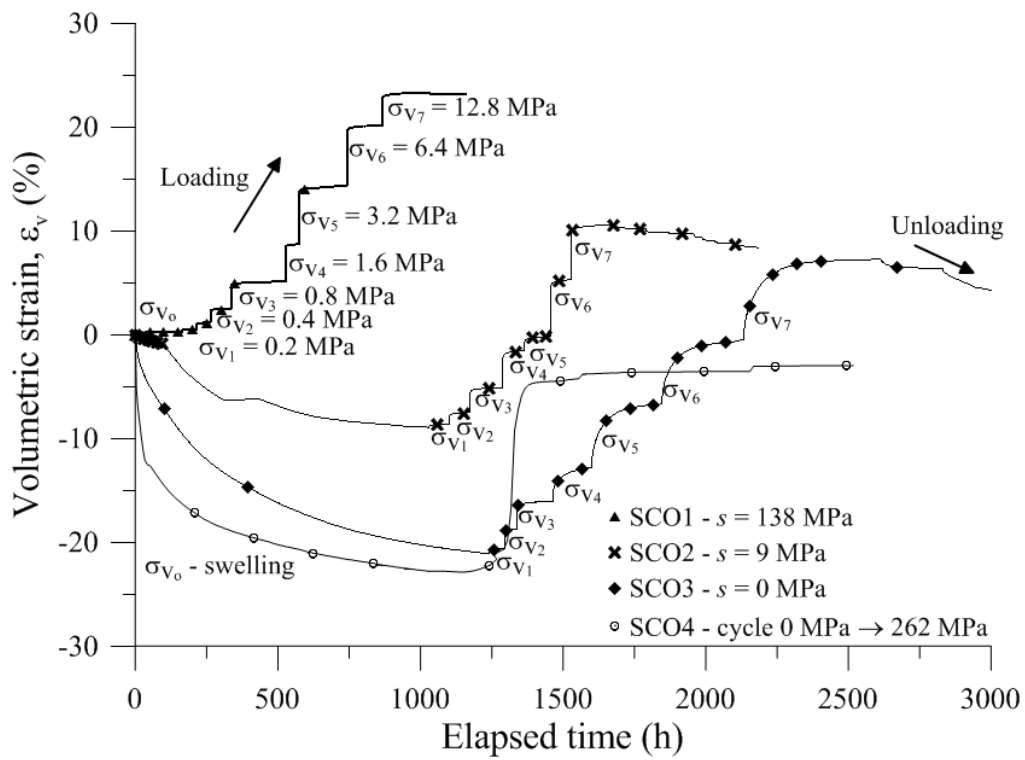


594

595 Figure 7. Imposed suctions by vapour equilibrium technique versus measured suction after
 596 equilibrium for the pellet/powder bentonite mixture.

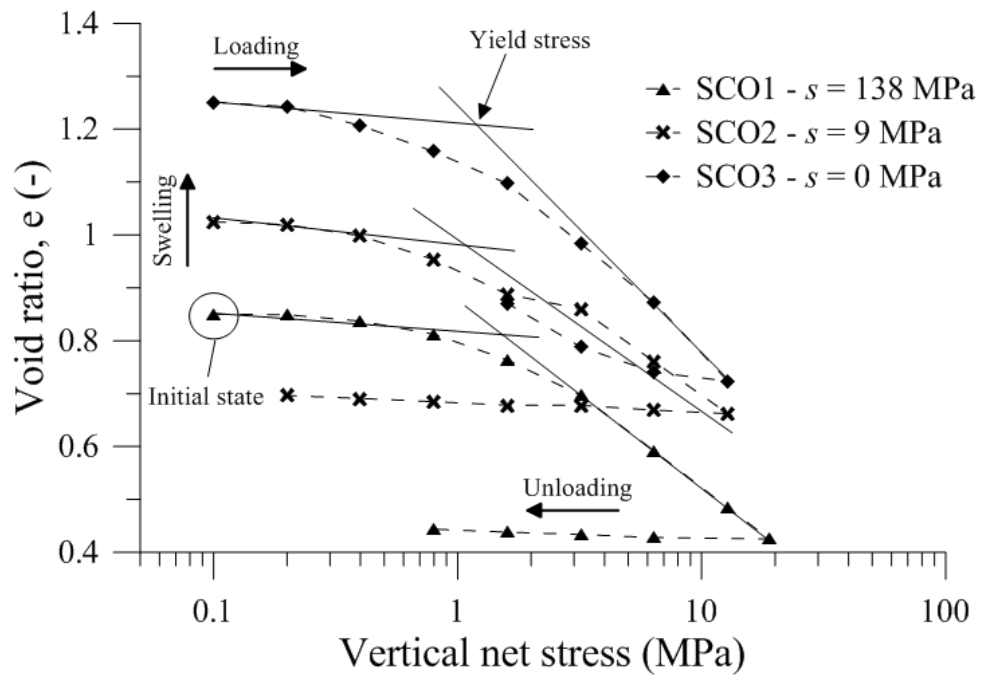
597

598



599

600 Figure 8. Evolution of the volumetric strain with time in the oedometer tests SCO1, SCO2
 601 and SCO3.

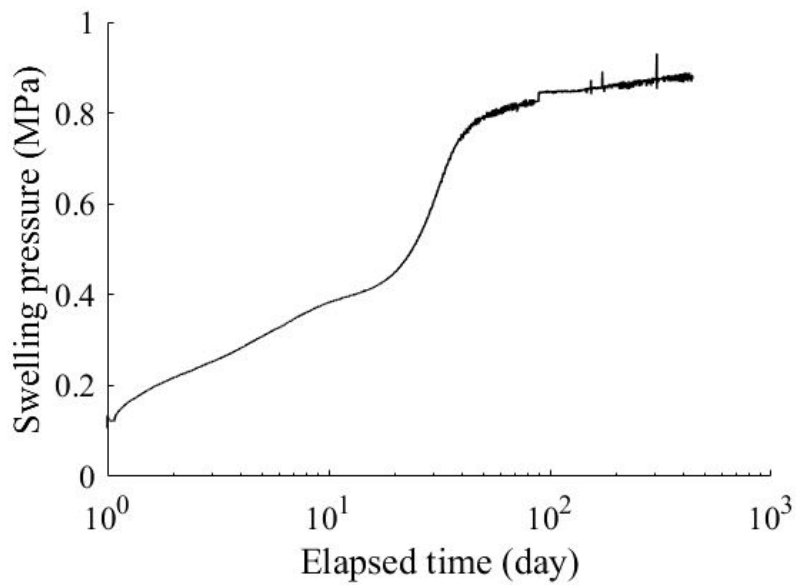


602

603

Figure 9. Void ratio versus vertical stress for tests SCO1, SCO2 and SCO3.

604

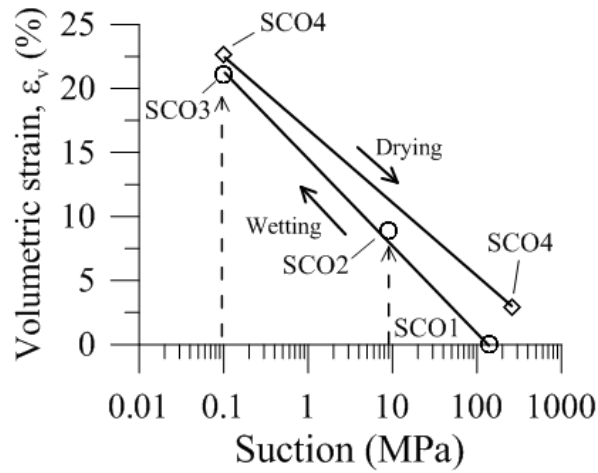


605

606

Figure 10. Evolution of axial swelling pressure with time in test CV1.

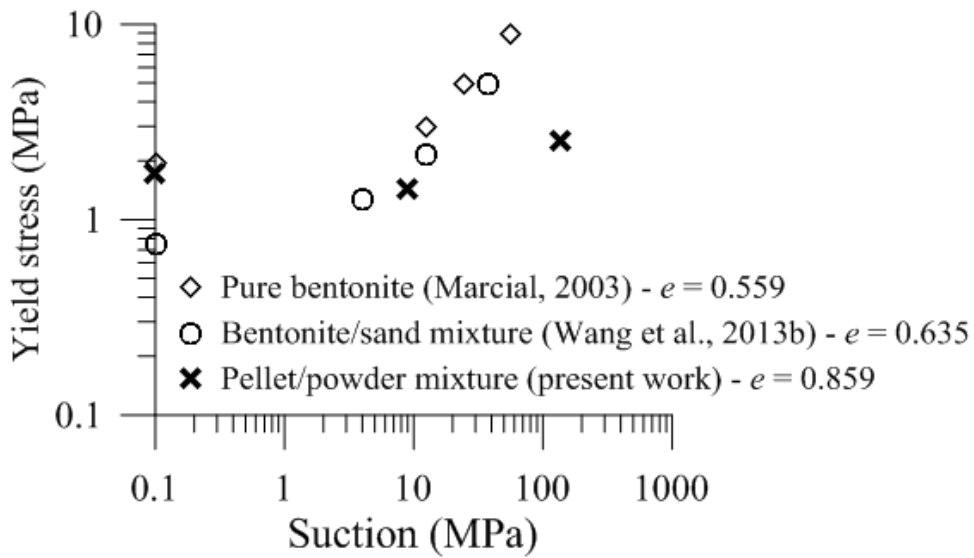
607



608

609 Figure 11. Volumetric strains measured at different suctions after equilibrium at the imposed
 610 suction for the different tests.

611



612

613 Figure 12. Yield stress versus suction for compacted bentonite with initial void ratio of 0.559
 614 (Marcial, 2003), compacted bentonite/sand mixture with initial void ratio of 0.635 (Wang et al.,
 615 2013b) and pellet/powder mixture with initial void ratio of 0.859 (present work).

616

617

618

619

620

621

622
623

Table 1. Test program for investigating the compressibility and swelling properties of pellet/powder bentonite mixture.

Test No.	Hydration condition	Suction (MPa)	Investigated property	Method
SCO1	Constant water content	138	Compressibility	-
SCO2	Vapor transfer	9	Compressibility	-
SCO3	Injected deionized water	0	Compressibility and swelling	Swell-consolidation
SCO4	Injected deionized water and vapor transfer	0 → 262	Swelling	-
CV1	Injected synthetic water	0	Swelling	Constant-volume

624

625

Table 2. Receipt for preparing the synthetic water.

Components	NaHCO ₃	Na ₂ SO ₄	NaCl	KCl	CaCl ₂ 2H ₂ O	MgCl ₂ O6H ₂ O	SrCl ₂ 6H ₂ O
Mass (g) per litre of solution	0.28	2.216	0.615	0.075	1.082	1.356	0.053

626